# Size-Controlled Synthesis of Magnetite Nanoparticles in the Presence of Polyelectrolytes

Satyabrata Si,[†] Atanu Kotal,[†] Tarun K. Mandal,*[,†] Saurav Giri,[‡,§] Hiroyuki Nakamura,[§] and Takao Kohara[§]

*Polymer Science Unit and Department of Solid State Physics, Indian Association for the Cultivation of Science, Jadavpur, Kolkata 700 032, India, and Graduate School of Material Science, University of Hyogo, Kamigori, Ako-gun, Hyogo 678-1297, Japan*

*Received May 19, 2004*

Magnetite nanoparticles of nearly uniform size have been prepared by precipitating ferrous ions in the presence of two different polyelectrolytes, viz., poly(acrylic acid) and the sodium salt of carboxymethyl cellulose at high pH (∼13). The size of the magnetite nanoparticles can be controlled easily by varying the concentration of the polyelectrolyte in the medium. Transmission electron microscopy study indicates that the average particle size varies from 5 to 15 nm, depending on the concentration and the nature of the polyelectrolyte. X-ray diffraction study shows the presence of only magnetite phase. FTIR spectroscopy and thermogravimetric analysis confirmed the presence of polyelectrolyte on the magnetite surface. The magnetization and Mössbauer studies were performed on two samples with mean diameters 7.0 and 14.7 nm. Magnetization measurements suggest that both of these particles are of single magnetic domain. The measurements also estimate the superparamagnetic blocking temperature, $T_B = 145$ K for smaller particles, while $T_B > 300$ K for the larger particles. Mössbauer spectra at 300 K show only a quadrupole doublet for the smaller particles and mostly a magnetically separated sextet for the larger ones, indicating also the marked size dependence of moment dynamics.

## Introduction

Nowadays shape- and size-controlled synthesis of magnetic oxide nanoparticles is of great technological and fundamental scientific importance. Magnetite ($Fe_3O_4$) is one of the phases of iron oxide that finds numerous applications due to its extraordinary magnetic and optical properties.[1] Magnetite has an inverse spinel structure where $O^{2-}$ ions are cubic close packed (ccp), the $Fe^{2+}$ ions are in octahedral sites, and the $Fe^{3+}$ ions are half in octahedral and half in tetrahedral sites.[2] Owing to its structure, magnetite is a typical semiconducting material, which is mainly found useful in various applications such as magnetic storage media,[3] printing inks,[4] magnetic resonance imaging,[5] drug delivery,[6] biomedicine,[7] biosensors,[8] magnetic refrigeration,[9] color imaging,[10] bioprocessing,[11] high-grade magnetic separation, and ferrofluids.[12] Conventional magnetic recording media have been fabricated by incorporating micrometer-sized iron oxide particles along with polymer/surfactant into a thin film. Recently there has been considerable interest in magneto-optic devices, which require magnetic particles of size below 10 nm. These small particles are optically transparent and ideal candidates for incorporation into ultrathin films of polymers.[13] Most of these technological and diagnostic applications also require magnetic particles of size smaller than 20 nm and a narrow size distribution. The physical and chemical properties of magnetic nanoparticles strongly depend on their size. Thus, the control over size and particularly size distribution without particle aggregation becomes a challenge for the fabrication of nanoscale devices and their use in bioanalytical applications.

* To whom correspondence should be addressed. Phone: 91−33−2473−4971. E-mail: psutkm@iacs.res.in.

[†] Polymer Science Unit, Indian Association for the Cultivation of Science.

[‡] Department of Solid State Physics, Indian Association for the Cultivation of Science.

[§] University of Hyogo.

(1) Yasumori, A.; Matsumoto, H.; Hayashi, S.; Okada, K. *J. Sol-Gel Sci. Techn.* **2000**, *18*, 249−258; Mamedov, A.; Ostrander, J.; Aliev, F.; Kotov, N. A. *Langmuir* **2000**, *16*, 3941−3949.

(2) Cornell, R. M.; Schwertmann, U. *The Iron Oxides: Structure, Properties, Reactions, Occurrence and Uses*; VCH: New York, 1996.

(3) Yamaguchi, K.; Matsumoto, K.; Fujii, T. *J. Appl. Phys.* **1990**, *67*, 4493.

(4) Peikove, V. T.; Jeon, K. S.; Lane, A. M. J. *J. Magn. Magn. Mater.* **1999**, *193*, 307.

(5) Oswald, P.; Clement, O.; Chambon, C.; Schouman-Claeys, E.; Frija, G. *Magn. Reson. Imaging* **1997**, *15*, 1025.

(6) Roullin, V. G.; Deverre, J. R.; Lemaire, L.; Hindre, F.; Julienne, M. C. V.; Vienet, R.; Benoit, J. P. *Eur. J. Pharm. Biopharm.* **2002**, *53*, 293.

(7) Fu, L.; Dravid, V. P.; Jhonson, D. L. *Appl. Surf. Sci.* **2001**, *181*, 173.

(8) Perez, J. M.; Simeone, F. J.; Saeki, Y.; Josephson, L.; Weissleder, R. *J. Am. Chem. Soc.* **2003**, *125*, 10192.

(9) McMichael, R. D.; Shull, R. D.; Swartzendruber, L. J.; Bennett, L. H.; Walson, R. E. *J. Magn. Magn. Mater.* **1992**, *111*, 29.

(10) Ziolo, R. F. In U.S. Patent No. 4474866, 1984.

(11) Nixon, L.; Koval, C. A.; Noble, R. D.; Slaff, G. S. *Chem. Mater.* **1992**, *4*, 117.

(12) Anton, A. I. *J. Magn. Magn. Mater.* **1990**, *85*, 137−140.

(13) Kang, Y. S.; Risbud, S.; Rabolt, J. F.; Stroeve, P. *Chem. Mater.* **1996**, *8*, 2209−2211.

10.1021/cm049205n CCC: $27.50 
Published on Web 07/31/2004

Magnetite is generally prepared mainly by three processes, viz., (1) coprecipitation of an aqueous solution of $Fe^{2+}/Fe^{3+}$ in the presence of a base, usually an alkali hydroxide or ammonia;[14,15] (2) thermal decomposition of an iron complex using an oxidizing agent;[16] and (3) by a sonochemical approach.[17] The particles have a large surface-area-to-volume ratio, which causes particle aggregation during particle formation through van der Waals or other force of attraction to reduce their surface energy. Consequently, several reports have been published on stabilizing these particles using different stabilizers such as a surfactant or a polymer matrix.[16,18−24] Among these reports a considerable amount of work has been executed where magnetite particles are first prepared and then stabilized using a stabilizer.[14,20,22,23] Recently, magnetic polystyrene nanoparticles have been prepared by the miniemulsion technique using presynthesized magnetite stabilized with oleic acid.[22] Lin et al. has reported the preparation of poly(acrylic acid)-coated $Fe_3O_4$ nanoparticles using this method.[23] Their particles show both ferro- and superparamagnetism. One of the main disadvantages of this method is that the particle size distribution can not be controlled, and also it is a time-consuming process. On the other hand, magnetite particles prepared in the presence of a stabilizer prevent particle coalescence during formation, resulting in a very small particle with narrow size distribution and in various sizes depending upon the experimental parameters. Therefore, many attempts have been made to synthesize magnetic nanoparticles in the presence of surfactants[16,25] or polymeric compounds with some specific functional groups as stabilizers.[24,26] For example, Sun et al. has synthesized 3−20 nm $Fe_3O_4$ nanoparticles using seed-mediated growth from a iron complex in organic phase at high temperature.[16] They have tuned the particle size using smaller particles as seeds. Superparamagnetic magnetite nanoparticles have also been prepared by solvothermal reduction in the presence of ethylene glycol, oleic acid, and trioctyl phosphine oxide or hexadecylamine.[27] Magnetite nanoparticles have also been successfully synthesized using poly(styrene acrylate) copolymer gel or porous sulfonated divinylbenzene copolymer as templates.[19,28] Among these polymers water-soluble polymeric stabilizers are very important, because the formed magnetic nanoparticles can be used in biomedical applications, as 98% of our body constituent is mainly water, besides other applications. Lee et al. has reported the synthesis of ultrafine $Fe_3O_4$ nanoparticles by coprecipitation of $Fe^{2+}/Fe^{3+}$ aqueous solution at high pH using poly(vinyl alcohol) (PVA) as a stabilizer without mentioning any particle size variation.[15] Although there are several reports on the synthesis of magnetite nanoparticles using polymer as a stabilizer, none of them refer to the preparation of magnetite nanoparticles in the presence of polyelectrolytes where particle size is controlled as a variable parameter.

Here we report a simple synthetic approach to prepare nearly monodisperse magnetite nanoparticles. We started from an aqueous solution of Fe(II) salt at high pH (∼13) and room temperature where two different water-soluble polymers, viz, poly(acrylic acid) (PAA) and sodium salt of carboxymethyl cellulose (NaCMC), have been used without any oxidizing/reducing agent. Size as well as the crystallinity of the magnetite nanoparticles were varied by preparing the particles at different polyelectrolyte concentration. The superparamagnetic and ferromagnetic features of magnetite nanoparticles were observed from the Mössbauer and magnetization studies, where magnetic properties strongly depend on the size of the particles.

## Experimental Section

**Materials.** Iron(II) sulfate heptahydrate ($FeSO_4$, $7H_2O$) (Merck, India) and sodium hydroxide (NaOH) (Merck, India) were used as received. Acrylic acid (Aldrich, 99%) was distilled under reduced pressure. The sodium salt of carboxymethyl cellulose (NaCMC) (British Drug House, London) was used without further purification. The viscosity-averaged molecular weight, and degree of substitution were determined earlier from this laboratory and were found to be $6.5 \times 10^4$ and 0.13, respectively.[29]

**Synthesis of Poly(acrylic Acid).** PAA was prepared in water at 70 °C by solution polymerization using 15% (w/v) acrylic acid and 0.1% (w/v) ammonium persulfate (APS) as initiator with constant nitrogen purging. After polymerization for 2 h, the polymer was precipitated into acetone and purified by dissolution in water and again reprecipitated into acetone. It was then dried at 60 °C for 48 h in a vacuum oven. The molecular weight of PAA was determined by a viscometric method in which intrinsic viscosity was measured using dioxane as the solvent at 30 °C. The viscosity-averaged molecular weight ($M_v$) was calculated using the following Mark−Houwink relation.

$$[\eta] = KM_v^a$$

The constant ($K = 76 \times 10^{-5}$dL/g and $a = 0.5$ for the solvent dioxane) in the above equation was obtained from the reference by Newman et al. where molecular weight was determined by the osmotic pressure method.[30] The molecular weight was found to be $1.5 \times 10^5$.

(14) Sahoo, Y.; Pizem, H.; Fried, T.; Golodnitsky, D.; Burstein, L.; Sukenik, C. N.; Markovich, G. *Langmuir* **2001**, *17*, 7907−7911.
(15) Lee, J.; Isobe, T.; Senna, M. *J. Colloid Interface Sci.* **1996**, *177*, 490.
(16) Sun, S.; Zeng, H. *J. Am. Chem. Soc.* **2002**, *124*, 8204−8505.
(17) Vijayakumar, R.; Koltypin, Y.; Felner, I.; Gedanken, A. *Mater. Sci. Eng. A* **2000**, *286*, 101−105.
(18) Zhou, Z. H.; Wang, J.; Liu, X.; Chan, H. S. O. *J. Mater. Chem.* **2001**, *11*, 1704−1709.
(19) Ziolo, R. F.; Giannelis, E. P.; Weinstein, B. A.; O'Horo, M. P.; Ganguly, B. N.; Mehrotra, V.; Russell, M. W.; Huffman, D. R. *Science* **1992**, *257*, 219−222; Rabelo, D.; Lima, E. C. D.; Reis, A. C.; Nunes, W. C.; Novak, M. A.; Garg, V. K.; Oliveira, A. C.; Morais, P. C. *Nano Lett.* **2001**, *1*, 105−108.
(20) Xie, G.; Zhang, Q. Y.; Luo, Z. P.; Wu, M.; Li, T. H. *J. Appl. Polym. Sci.* **2003**, *87*, 1733−1738.
(21) Wang, L. W.; Teng, X.; Wang, J. S.; Yang, H. *Nano Lett.* **2003**, *3*, 789.
(22) Ramirez, L. P.; Landfester, K. *Macromol. Chem. Phys.* **2003**, *204*, 22−31.
(23) Lin, Y. J.; Wang, L.; Lin, J. G.; Huang, Y. Y.; Chiu, W. Y. *Synth. Met.* **2003**, *135−136*, 769−770.
(24) Lin, H.; Watanabe, Y.; Kimura, M.; Hanabusa, K.; Shirai, H. *J. Appl. Polym. Sci.* **2003**, *87*, 1239−1247.
(25) Fried, T.; Shemer, G.; Markovich, G. *Adv. Mater.* **2001**, *13*, 1158.
(26) Lee, D. K.; Kang, Y. S.; Lee, C. S.; Stroeve, P. *J. Phys. Chem. B* **2002**, *106*, 7267−7271; Jones, F.; Colfen, H.; Antonietti, M. *Colloid Polym. Sci.* **2000**, *278*, 491−501.
(27) Hou, Y.; Yu, J.; Gao, S. *J. Mater. Chem.* **2003**, *13*, 1983.
(28) Qu, S. C.; Yang, H. B.; Ren, D. W.; Kan, S. H.; Zou, G. T.; Li, D. M.; Li, M. H. *J. Colloid Interface Sci.* **1999**, *215*, 190−192.
(29) Banerjee, P. *Eur. Polym. J.* **1998**, *34*, 841−847.
(30) Newman, S.; Krigbaum, W. R.; Laugier, C.; Flory, P. J. *J. Polym. Science* **1954**, *14*, 451.

**Synthesis of Magnetite Nanoparticles.** An aqueous solution of $FeSO_4 \cdot 7H_2O$ (10 mL, 0.1 M) was added dropwise to a 10 mL aqueous solution of 2% (w/v) PAA with continuous stirring. The final concentration of the polymer in the medium was 1% (w/v). The mixture was stirred for 30 min to complete the formation of the iron−polymer complex. The pH of the solution was then increased slowly by adding 0.1 M NaOH solution. The reaction mixture was subsequently aged for 1 h with constant stirring. The process was repeated with varying the concentration of PAA, viz., 0.75%, 0.50%, and 0.25% (w/v), respectively, for preparing size-variable magnetite nanoparticles. Different size magnetite nanoparticles were also synthesized by varying the concentration of NaCMC using a reaction procedure similar to that described above. After the reaction, excess polyelectrolyte was removed by centrifugation followed by washing with double distilled water. This purification process was repeated three times. The resultant solid magnetite materials are then dried in a vacuum oven at 60 °C for 24 h. All the experiments were performed from dry polymer-coated magnetite sample after removing excess unadsorbed polyelectrolytes, except in the case of transmission electron microscopy (TEM).

**Characterization.** TEM samples were prepared by putting a drop of the as-prepared magnetite suspension on a carbon-coated copper grid and then dried in air. The dried grid was then placed under a JEOL JEM-200CX transmission electron microscope. The images were taken at an acceleration voltage of 120 kV.

The attachment of the polymer on the magnetite particle surface was confirmed by Fourier-transform infrared spectroscopy (FTIR). FTIR spectra of the polymer-coated magnetite nanoparticles were recorded from KBr pellets prepared by mixing dry, coated nanoparticles with KBr in a Series II Nicolet Magna-IR 750 spectrometer.

The crystallite phase was identified by recording X-ray powder diffraction patterns (XRD) of the dry, purified samples using a Philips PW 1830 diffractometer equipped with a Cu Kα radiation source.

The amount of polyelectrolyte adsorbed on the magnetite nanoparticles was determined by a thermogravimetric analyzer (TGA) using a Mettler Toledo Star System TGA/SDTA851e in the presence of $N_2$ gas with a heating rate of 20 °C/min.

The Mössbauer spectrum was recorded in a transmission geometry using a ∼1 GBq $^{57}Co$ source in a Rh matrix with a Wissel velocity drive unit in a constant acceleration mode. The Mössbauer parameters were estimated with respect to α-Fe.

The magnetization study was performed using a SQUID magnetometer (Quantum Design MPMS-5).

## Results and Discussion

First of all, we would like to discuss the chemistry of the formation of magnetites. $Fe_3O_4$ is generally prepared via coprecipitation of $Fe^{2+}$ and $Fe^{3+}$ ions by a base following this chemical reaction:[31]

$$Fe^{2+} + 2Fe^{3+} + 8OH^- \rightarrow Fe_3O_4 + 4H_2O \qquad (1)$$

According to the results of thermodynamic modeling of this system, a complete precipitation of $Fe_3O_4$ is expected in the pH range 7.5−14, while mainly the molar ratio of $Fe^{2+}$ and $Fe^{3+}$ is 1:2. The mixture of $Fe^{2+}/Fe^{3+}$ ions with a mole ratio of 1:1 has also been used to prepare magnetite.[32] Magnetite can also be formed by controlled oxidation of a $Fe^{2+}$ ion solution according to the following equations:

$$3Fe^{2+} + 4H_2O \rightarrow Fe_3O_4 + 6H^+ + 6H_2 \qquad (2)$$

$$Fe^{2+} + O_2 + OH^- \rightarrow Fe_3O_4 + H^+ \qquad (3)$$

As described above there are two possible methods for magnetite preparation. First, according to the eq 1, the formation of magnetite requires both ferrous and ferric ion. However, in our case, magnetite nanoparticles were prepared only from $Fe^{2+}$ ion in the presence of polyelectrolyte in air at high pH. It is well-known that $Fe^{2+}$ ion can be oxidized easily by oxygen in the air. As a matter of fact, the ferrous ions that we have used contain some ferric ions, and during stirring with the polymer, presumably some of the ferrous ions are oxidized to ferric ions by oxygen in the air. The color of the iron−polymer complex changed from light green to yellow-orange, indicating oxidation of $Fe^{2+}$ to $Fe^{3+}$ under air. When NaOH was added, the color of the solution changed from yellow-orange through green to black-red, indicating the formation of magnetite in the presence of air, and it was quite stable. To study the effect of atmospheric oxygen on the formation of magnetite nanoparticles, we have performed the same reaction in the presence of nitrogen gas. In this case, the color of the iron−polymer complex also changed to yellow-orange, because our original ferrous sample contains a small amount of ferric ion, as we mentioned previously. The yellow-orange color changed to green upon NaOH addition. However, it was remained green while the nitrogen flow was maintained through the medium. When this solution was exposed to air, the color changed to brown and precipitated immediately. Second, magnetite may also be formed following eqs 2 and 3. The formation mechanism of magnetite in our case is still unclear.

Figure 1 shows the transmission electron micrograph of all the PAA-coated $Fe_3O_4$, and Figure 2 shows the CMC-coated $Fe_3O_4$ prepared by varying the polymer concentration. All the samples show that there is nearly uniform distribution of particle size with high particle density. Table 1 shows the variation of particle size with polyelectrolyte concentration, determined by measuring the size of at least 100 particles from the respective TEM picture. It clearly indicates that there is a continuous increase of particle size upon decreasing the concentration of PAA as well as NaCMC. The relative standard deviation ($\sigma_r$)[33] values reveal that the magnetite nanoparticles prepared at high polyelectrolyte concentration are relatively more monodisperse than the particles prepared at low concentration. The nanoparticles are generally considered to be monodisperse, if the standard deviation ($\sigma$)[34] ≤ 5% relative to the average size, i.e., the value of $\sigma_r$ lies within 5 for spherical particles. Furthermore, CMC-coated $Fe_3O_4$ nanoparticles show more monodispersity compared to the magnetite particle prepared with PAA. However, in the case of PAA, the variation of particle size with increasing PAA concentration is more prominent than for the particles prepared by varying NaCMC concentration. In

(31) Kim, D. K.; Mikhaylova, M.; Zhang, Y.; Muhammed, M. *Chem. Mater.* **2003**, *15*, 1617−1627.

(32) Godovsky, D. Y.; Varfolomeev, A. V.; Efremova, G. D.; Cherepanov, V. M.; Kapustin, G. A.; Volkov, A. V.; Moskvina, M. A. *Adv. Mater. Opt. Electron.* **1999**, *9*, 87.

(33) The relative standard deviation of the size distribution was calculated from the equation $\sigma_r = 100 \times \sigma/D$, where $\sigma$ is the standard deviation and $D$ is the average diameter of particles.

(34) The standard deviation of the size distribution was calculated from the equation $\sigma = [\sum n_i(D_i - D)^2/(N-1)]^{0.5}$, where $n_i$ is the number of particles having diameter $D_i$. $D$ is the average diameter $[=(\sum n_i D_i)/N]$, and $N$ is the total number of particles.

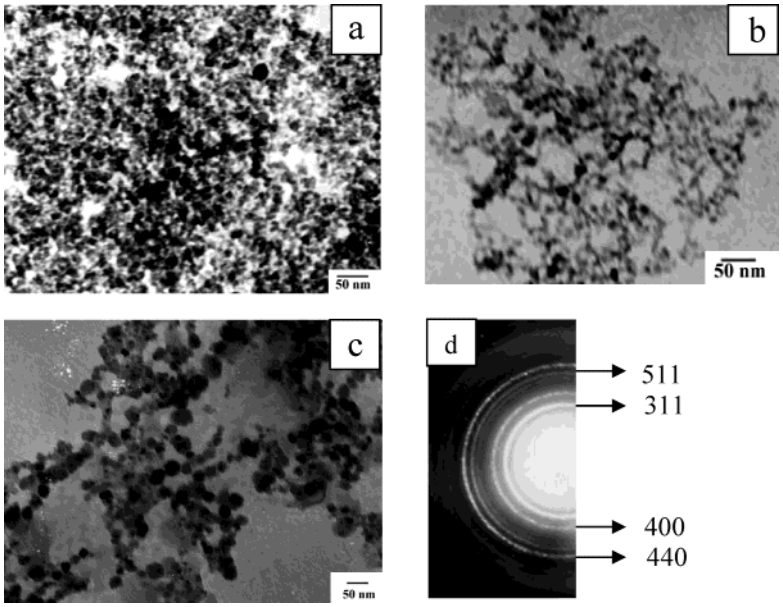


**Figure 1.** TEM pictures of the as-prepared PAA-coated $Fe_3O_4$ nanoparticles prepared with various PAA concentrations: (a) 1%, (b) 0.5%, (c) 0.25% (w/v). (d) Selected portion of the electron diffraction pattern of PAA-$Fe_3O_4$ nanocomposite prepared in the presence of 1% PAA.

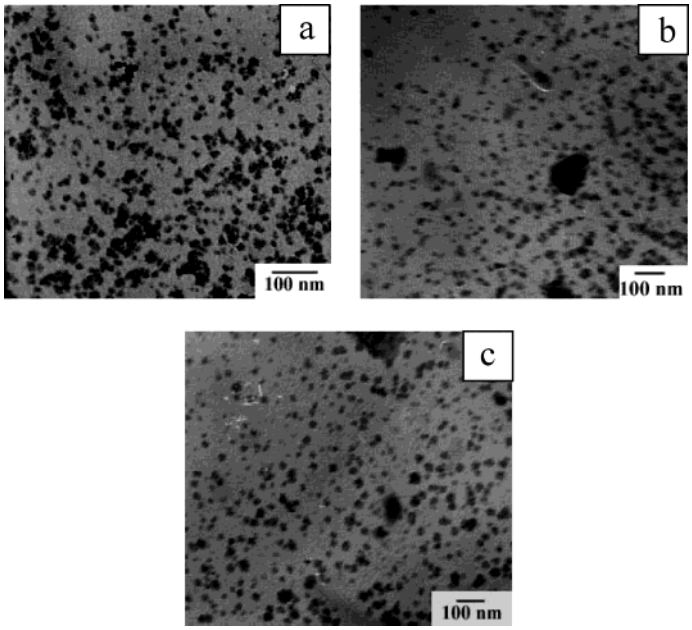


**Figure 2.** TEM pictures of the as-prepared CMC-coated $Fe_3O_4$ nanoparticles prepared with various NaCMC concentrations: (a) 1%, (b) 0.5%, and (c) 0.25% (w/v).

**Table 1. Average Particle Size of Magnetite Nanoparticles Prepared by Varying Polyelectrolyte Concentration**

| polyelectrolyte | concn, %, w/v | mean diameter, nm | SD ($\sigma$) | rel SD ($\sigma_r$) | particle size from Scherer's equation, nm |
|---|---|---|---|---|---|
| PAA | 1.00 | 5.1 | 0.42 | 8.2 | 4.9 |
| NaCMC | | 10.5 | 0.06 | 0.6 | 6.6 |
| PAA | 0.50 | 7.0 | 0.58 | 8.3 | 5.8 |
| NaCMC | | 14.4 | 0.92 | 6.4 | 16.5 |
| PAA | 0.25 | 14.7 | 4.20 | 28.5 | 9.5 |
| NaCMC | | 15.5 | 1.20 | 7.7 | 16.7 |

the case of NaCMC, magnetite nanoparticles were obtained with a minimum diameter of 10 nm, while the size of magnetite nanoparticles obtained using PAA was up to 5 nm. The electron diffraction (ED) pattern of some selected portion of magnetite nanoparticles prepared with 1% PAA in Figure 1d indicates that all the rings are clear and well-defined, which reveals the nanocrystallinity of rather uniform crystallite size.[18] The formation of uniform magnetite nanoparticles can be attributed to the attachment of the polyelectrolyte on the surface of the particles. The existence of polyelectrolytes thus prevents the coalescence of particles due to the repulsive interaction between the same charges on the polyelectrolytes. Thus, the concentration of the polyelectrolyte plays an important role in the preparation of uniform and size-controlled nanoparticles. In the case of higher PAA concentration, magnetite nanoparticles show a relatively better monodispersity. At lower PAA concentration, the amount of PAA adsorbed on the magnetite particle surface is lower, which causes an increased chance of coalescence between nanoparticles,

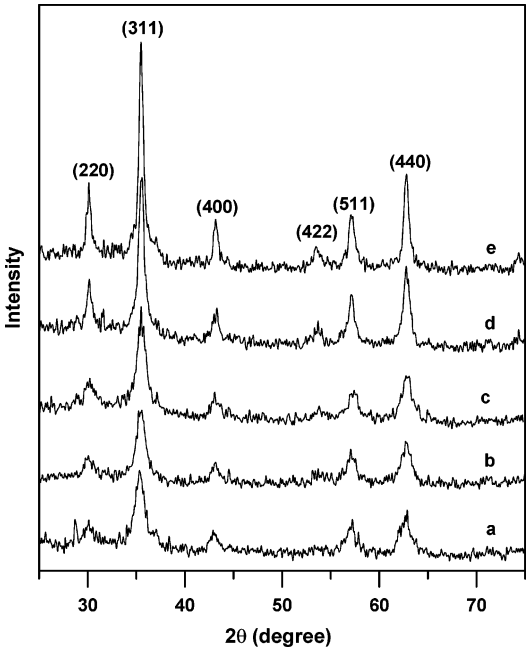


**Figure 3.** X-ray diffraction pattern of PAA-$Fe_3O_4$ nanocomposites prepared with (a) 1%, (b) 0.75%, (c) 0.5%, (d) 0.25%, and (e) 0% (w/v) of PAA.

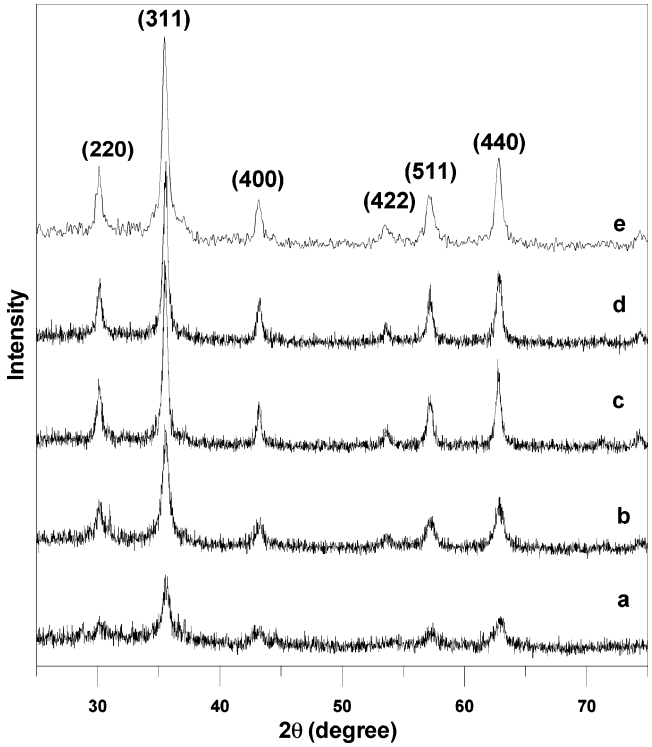


**Figure 4.** X-ray diffraction pattern of CMC−$Fe_3O_4$ nanocomposites prepared with (a) 1%, (b) 0.75%, (c) 0.5%, (d) 0.25%, and (e) 0% (w/v) of NaCMC.

resulting in a broad distribution of particle size. As shown in Table 1, the highest value of the $\sigma_r$ depicted is for the 0.25% PAA. CMC-coated $Fe_3O_4$ nanoparticles also show similar kind of behavior.

The iron oxide phase was identified from the XRD pattern, as shown in Figures 3 and 4, with peak positions at 30.00 (220), 35.5 (311), 43.1 (400), 53.4 (422), 57 (511), and 63 (440), which are consistent with the standard data for magnetite.[15,18] Figures 3 and 4 show that there is continuous broadening of each peak with the increase in PAA or NaCMC concentration. The XRD peak broadening is therefore attributed to the decrease in the particle size.[15] This can be verified quantitatively using Scherer's equation,[35] which gives a relationship between peak broadening in XRD and particle size. The particle sizes estimated by this equation are given in Table 1. These values confirm that the peak broadening in the XRD trace with increasing polyelectrolyte concentration is due to the decrease in particle size, although there is some deviation in the particle sizes compared to that measured by TEM (see Table 1), which is due to the use of two different techniques for the measurements of the size of the particles.[36] From Figure 3, it is clear that the relative XRD peak intensity decreases with increasing PAA concentration, which indicates that the relative crystallinity of the magnetite decreased. The XRD pattern of CMC-coated magnetite nanoparticles also shows a similar decreasing trend with increasing NaCMC concentration, as displayed in Figure 4. Besides magnetite peaks, we did not observe any other peak in the diffraction pattern for all the samples.

The attachment of the polymer on the particle surface was confirmed by FTIR spectroscopy. The characteristic stretching frequencies of PAA at low pH include O−H stretching at ~3431 $cm^{-1}$; C═O stretching at 1728 $cm^{-1}$, and the C−O stretching at 1100−1200 $cm^{-1}$. At high pH, PAA shows peaks at 1562 and 1408 $cm^{-1}$ due to carboxylate ($COO^-$) asymmetric and symmetric stretching, respectively.[37] There is no absorption peak in the region of C═O for PAA−magnetite nanocomposites (Figure 5a,b). However, parts a and b of Figure 5 show the peaks around 1549 and 1397 $cm^{-1}$, which are due to asymmetric and symmetric stretching of the $COO^-$, respectively, along with a peak at 1114 $cm^{-1}$ for the C−O stretching of PAA in the composite. This observation suggested that the PAA chains were anchored on the magnetite particle surface involving bidentate chelation of carboxylate ion of PAA at high pH. The peak position for carboxylate asymmetric and symmetric stretching of neat NaCMC was found to be 1622 and 1421 $cm^{-1}$, respectively (Figure 5c). Spectra for CMC-coated magnetite particles (Figure 5d,e) reveal bands at 1592 and 1411 $cm^{-1}$, corresponding to characteristic asymmetric and symmetric stretching of carboxylate, respectively, indicating that CMC chains are also attached in a similar fashion on the magnetite surface. In both cases, the position of the carboxylate asymmetric and symmetric stretching frequency is slightly blue shifted when attached to the magnetite particle surface compared to the unadsorbed PAA at high pH and NaCMC. This may be attributed to the decrease in force constant resulting from the inhibition of conjugation of $COO^-$ when attached to a particle surface. In the unbound caboxylate ion, the C−O bond has partial double bond character and hence the force constant is greater, causing absorption at higher wavenumber.

The attachment of the polyelectrolyte on the magnetite particle surface was further confirmed by TGA. In

(35) Cullity, B. D. In *Elements of X-ray Diffractions*; Addition-Wesley: Reading, MA, 1978; p 102.
(36) Bandyopadhyay, S.; Paul, G. K.; Roy, R.; Sen, S. K.; Sen, S. *Mater. Chem. Phys.* **2002**, *74*, 83−91.
(37) Kirwan, L. J.; Fawell, P. D.; Bronswijk, W. V. *Langmuir* **2003**, *19*, 5802.

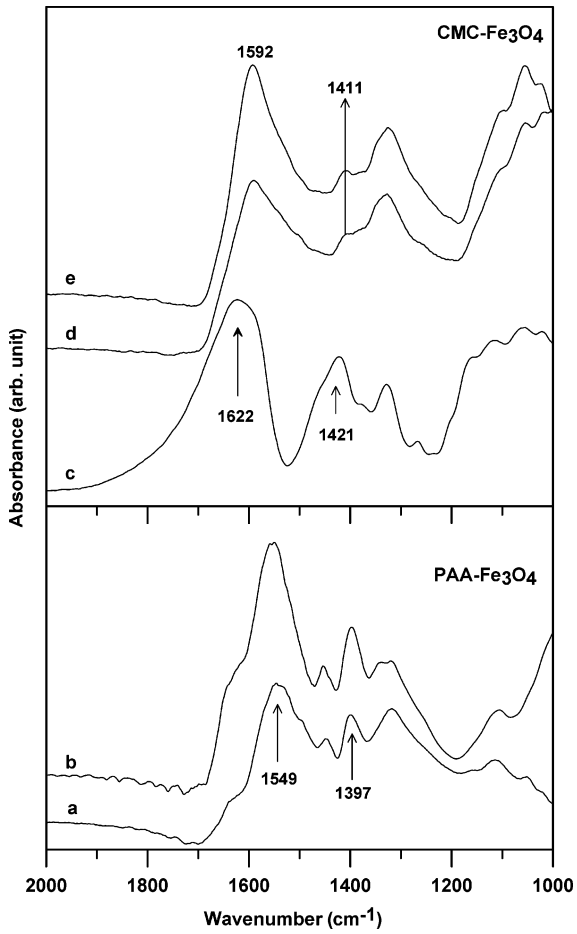


**Figure 5.** FTIR spectra of (a) $Fe_3O_4$ prepared with 0.5% PAA, (b) $Fe_3O_4$ prepared with 1% PAA, (c) pure NaCMC, (d) $Fe_3O_4$ prepared with 0.25% NaCMC, and (e) $Fe_3O_4$ prepared with 1% NaCMC.

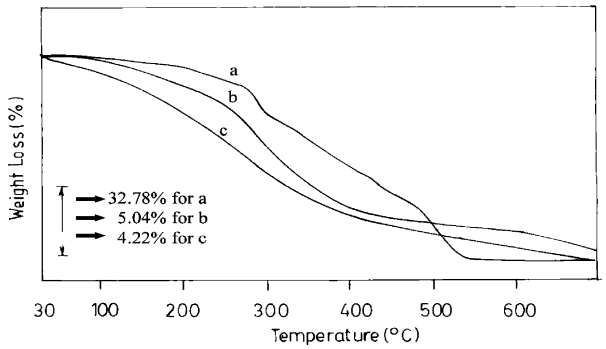


**Figure 6.** TGA thermograms of (a) pure PAA and PAA−$Fe_3O_4$ nanocomposites prepared by employing (b) 1% PAA and (c) 0.25% PAA.

case of PAA-coated magnetite, TGA thermograms show a continuous weight loss in the temperature range of 200−550 °C, which is the range of decomposition temperature for PAA (compare parts a and b of Figure 6). Similarly, decomposition of CMC-coated magnetite nanoparticles started at 250 °C and ended at 650 °C, which is the decomposition temperature range for NaCMC (Figure 7). All the TGA were performed under nitrogen atmosphere to minimize the mass increase due to iron oxidation and allowed the polymer to decompose thermally. In both the cases, it was observed that the percentage of weight loss is more when the magnetite is prepared at high polymer concentration compared to

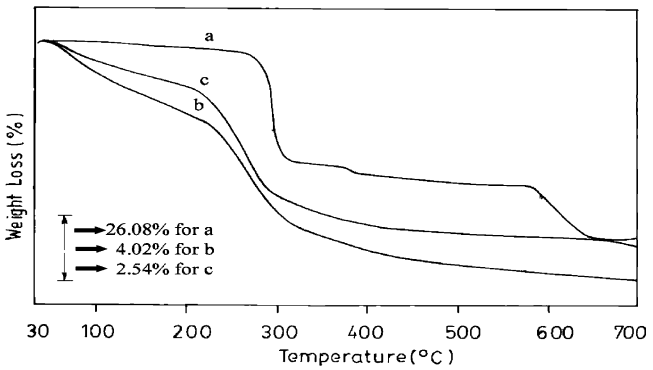


**Figure 7.** TGA thermograms of (a) pure NaCMC and CMC−$Fe_3O_4$ nanocomposites prepared by employing (b) 1% NaCMC and (c) 0.25% NaCMC.

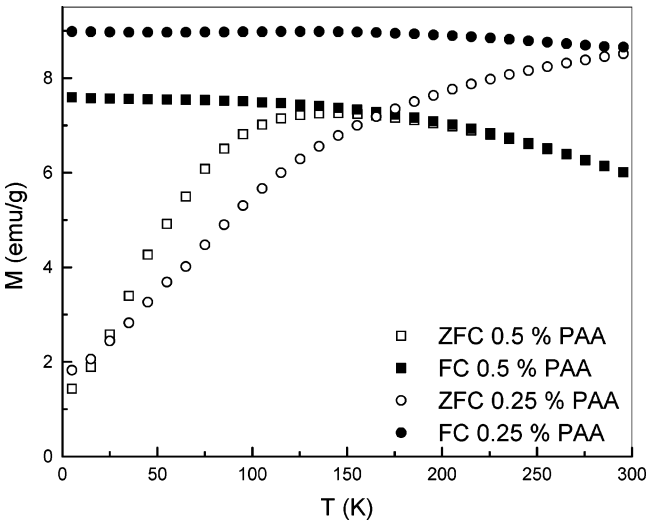


**Figure 8.** Temperature dependence of magnetization measured under field-cooled (FC) and zero-field-cooled (ZFC) conditions for the samples prepared with 0.50% and 0.25% PAA. The applied field was 0.01 T.

that formed at low polymer concentration. Again, we know from the TEM study that the particle size is smaller when the magnetites are prepared with high polymer concentration. The particles with small size have a large surface area that can adsorb a large amount of polymer on the surface, and hence, the chance of weight loss is greater and vice versa. Therefore, as the particle size is increased with lowering the polymer concentration, there is a decrease in the percentage of weight loss.

The magnetization study was performed on the samples prepared with 0.50% and 0.25% PAA with mean diameter $D = 7.0$ and 14.7 nm, respectively. The magnetization measured at 0.01 T, shown in Figure 8, exhibits the field-cooled effect. ZFC (zero-field-cooled) curves were obtained by cooling the sample under zero magnetic field and then measured by applying 0.01 T in the heating cycle. FC (field-cooled) curves were obtained like in the ZFC experiment, though samples were cooled to the lowest temperature under 0.01 T. In case of sample with $D = 14.7$ nm, ZFC and FC curves do not coincide up to 300 K. On the other hand, ZFC and FC curves depart from each other below ∼235 K for the sample with $D = 7.0$ nm. In the case of magnetic nanoparticles, the maximum in the ZFC curve is characterized in general as the blocking temperature

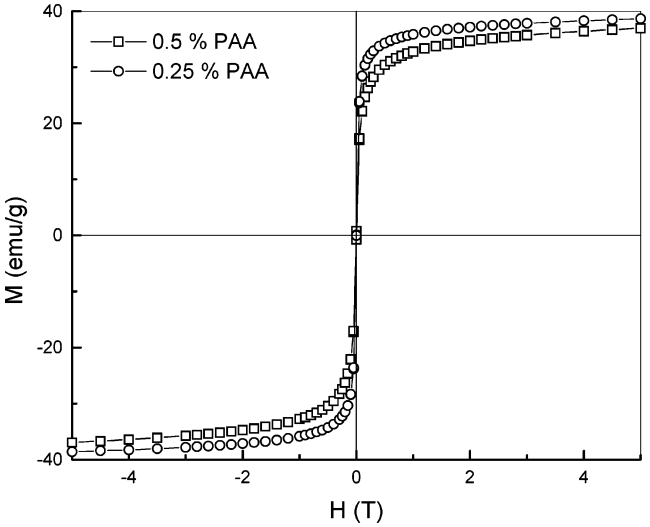


**Figure 9.** Magnetization curves for the samples prepared with 0.50% and 0.25% PAA at 295 K.

($T_B$) of the superparamagnet, i.e., an assembly of magnetically aligned moments in a single-domain fine particle. A broadened peak in the ZFC curve is observed for the case of $D = 7.0$ nm, while no peak is noticed up to 300 K for $D = 14.7$ nm. If the interparticle magnetic interaction is weak, $T_B$ can be related as $K_{an}V = 25k_BT_B$ for a random distribution of a single domain magnetic particle.[38] Here, $V$ and $K_{an}$ are the volume and the anisotropy energy density constant of the particle, respectively. Considering $T_B \approx 145$ K for the sample with $D = 7.0$ nm, the value of $K_{an}$ is estimated to be $\sim 2.8 \times 10^5$ J/m$^3$, which is close to those found in the literature for $Fe_3O_4$ nanoparticles.[39] The large anisotropy is explained by several intrinsic factors of the nanoparticle, which mainly include magnetocrystalline, surface, and shape anisotropy for noninteracting single domain nanoparticles. In case of a small magnetic particle, the interparticle interaction in general helps to agglomerate the particles. These agglomerated nanoparticles act as a cluster, resulting in the increase of $T_B$. In case of the sample with $D = 14.7$ nm, the superparamagnetic blocking temperature was not observed up to 300 K, indicating the effect of such agglomeration, which has also been observed in TEM results.

Magnetization curves measured at 295 K, which are shown in Figure 9, show almost immeasurable coercivity and remanance, suggesting that these nanoparticles are of a single domain. In case of no hysteresis, the average size of the particle can be estimated from the initial susceptibility, $\chi_i = (dM/dH)_{H\to 0}$, coming mainly from the largest particles. An upper limit for the magnetic size, $D_m$, may be estimated using the formula[40]

$$D_m = \frac{18k_BT}{\pi}\frac{\chi_i}{\rho M_s^2} \qquad (4)$$

where $\rho$ is the density of $Fe_3O_4$ (5.18 g/cm$^3$). The value

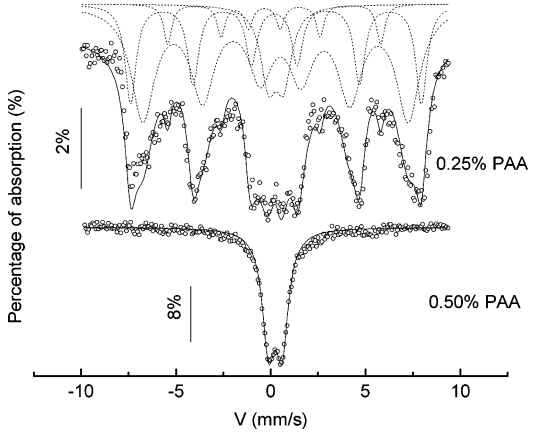


**Figure 10.** Mössbauer spectra of $Fe_3O_4$ nanoparticles prepared in the presence of 0.25% and 0.50% PAA at 300 K. The solid curves indicate the fitting of the Mössbauer spectra. The broken curves indicate deconvoluted components of the fitting of the Mössbauer spectrum for sample prepared with 0.25% PAA.

of $\chi_i$ was determined to be $34.3 \times 10^{-3}$ and $47.5 \times 10^{-3}$ emu/g, respectively. Using the value of saturation magnetization, $M_s$, obtained from the magnetization curve, the values of $D_m$ were estimated to be ~9 and ~13 nm for the samples with $D = 7.0$ and 14.7 nm, respectively, indicating good accordance of particle sizes estimated from magnetization and TEM experiments.

A Mössbauer study has been incorporated on the same samples used for the magnetization studies. Mössbauer spectra for those samples measured at 300 K are shown in Figure 10, exhibiting different features. Only a symmetric quadrupole doublet is observed for $D = 7.0$ nm. On the other hand, the spectrum for $D = 14.7$ nm exhibits the superposition of a quadrupole doublet and magnetically separated sextet, although the sextet involves a minor contribution of α-Fe besides the patterns expected for $Fe_3O_4$. The estimated values of the internal magnetic fields are $47.7 \pm 0.10$ and $43.5 \pm 0.25$ T, corresponding to the tetrahedral and octahedral sites, respectively; iron ions in the spinel $Fe_3O_4$ are distributed in two sites, and the resultant Mössbauer spectrum is a superposition of two sextets wherein the line from the octahedral site is broadened owing to electron transfer between $Fe^{2+}$ and $Fe^{3+}$. The values of the internal fields are 50.3 and 48.0 T at the tetrahedral and octahedral sites, respectively, for the bulk $Fe_3O_4$ compound.[41] The reduction of the internal magnetic field with respect to the bulk counterpart is not so unlikely for magnetic nanoparticles.[42] As seen in Figure 10, another sextet pattern corresponding to the α-Fe phase with internal field $\sim 33.0 \pm 0.3$ T, which is close to the value for bulk α-Fe,[41] has also been detected for the sample with $D = 14.7$ nm. The fraction of α-Fe phase was estimated to be ~7% from the intensity, assuming the common Debye−Waller factor. The lack of XRD peaks corresponding to α-Fe may be due to the small fraction of α-Fe. Moreover, the XRD peak intensities may be decreased considerably due to line broadening. Iron nanoparticles are strongly pyrophoric and are

(38) Dorman, J. L. *Revue Phys. Appl.* **1981**, *16*, 275.
(39) Balcells, L.; Iglesias, O.; Labarta, A. *Phys. Rev. B* **1997**, *55*, 8940; Jonsson, T.; Mattsson, J.; Djurberg, C.; Khan, F. A.; Nordblad, P.; Svedlindh, P. *Phys. Rev. Lett.* **1995**, *75*, 4138; Luo, W.; Nagel, S. R.; Rosenbaun, T. F.; Rosensweig, R. E. *Phys. Rev. Lett.* **1991**, *67*, 2721.
(40) Carpenter, E. E. *J. Magn. Magn. Mater.* **2001**, *225*, 17.
(41) Greenwood, N. N.; Gibb, T. C. In *Mossbauer Spectroscopy*; Chapman and Hall Ltd.: London, 1971; p 251.
(42) Giri, S.; Ganguly, S.; Bhattacharya, M. *Appl. Surf. Sci.* **2001**, *182*, 345.

easily oxidized in the presence of a trace amount of oxygen. This oxidation process starts at the surface of the particles. In such a case, α-Fe is suggested to exist in the core of the particle, as discussed in the literature.[42,43] In case of the sample with $D = 14.7$ nm, the doublet contribution is estimated to be ∼12%, assuming the common Debye−Waller factor. The quadrupole splitting and isomer shift for the doublet are estimated to be $0.56 \pm 0.05$ and $\sim 0.39 \pm 0.05$ mm/s, respectively, and those for the sample with $D = 7.0$ nm are $0.70 \pm 0.02$ and $0.36 \pm 0.02$ mm/s, respectively. For both the cases, the values of isomer shift are close to those found in other $Fe_3O_4$ nanoparticles.[44] The isomer shift is typically ≥1.0 mm/s for $Fe^{2+}$ while ∼0.3−0.4 mm/s for $Fe^{3+}$. The present value suggests that the average valence is closer to $Fe^{3+}$.

In the case of the nanoparticle, the magnetic anisotropy energy ($E$) is often close to the thermal excitation energy, resulting in the fast fluctuation of the localized moment. The relaxation time is given by $\tau_{fluc}(T) = \tau_0 \exp(E/k_BT)$,[45,46] where $\tau_0$ is on the order of $10^{-10}-10^{-13}$s and only weakly dependent on temperature,[46] and $k_B$ is the Boltzmann's constant. This results in the relaxation of the superparamagnet in magnetic nanoparticles. In such a case, the observed magnetic feature depends on the time scale of observation of the experiment ($\tau_{obs}$). In case of the Mössbauer study, if $\tau_{fluc} \gg \tau_{obs}$ at a particular temperature, the sextet pattern characteristics for the ordered state is observed. When both the time scales becomes comparable, features of superparamagnetic relaxation start appearing initially by reducing the splitting of the sextet pattern. The reduction of magnetic splitting for $D = 14.7$ nm with respect to the bulk counterpart may be related to the above feature. In the extreme case where $\tau_{fluc} \ll \tau_{obs}$ at a particular temperature, the sextet pattern turns to a quadrupole doublet or singlet. The observation of only a doublet pattern for $D = 7.0$ nm thus indicates the feature of superparamagnetic relaxation. On the other hand, for $D = 14.7$ nm the broad magnetic sextet coexists with the quadrupole doublet, which is suggested to appear due to the large distribution of particle size, as noticed from the TEM observation (Table 1).

## Conclusions

In conclusion, relatively monodisperse magnetite nanoparticles of various sizes have been synthesized from iron(II) ions singly in the presence of two polyelectrolytes, PAA and NaCMC. The particle size could be varied by changing the concentration of the polyelectrolytes. From a FTIR study we were able to verify and classify the type of attachment of the electrolyte to the particles. The magnetization and Mössbauer studies were performed on two samples with 0.25% and 0.50% PAA having mean diameters 7.0 and 14.7 nm, respectively. Magnetization measurements suggest that both of these particles are of single magnetic domain. The superparamagnetic blocking temperature $T_B = 145$ K was observed for smaller particles, while $T_B > 300$ K was seen for the larger particles. Mössbauer spectra at 300 K show only a quadrupole doublet for the smaller particles, while mostly a magnetically separated sextet is observed for the larger ones, although the latter consists of a minor contribution from the doublet. These results indicate that the dynamical nature of magnetization is strongly size-dependent, namely, coupled moments in the smaller particles fluctuate dynamically at room temperature like a superparamagnet, while those in the larger particles are mostly static, although the dynamical component seems to be also involved in the latter, due to the large distribution of particle size.

**Acknowledgment.** S.S. thanks the Council of Scientific and Industrial Research, Government of India for providing a junior research fellowship. This work was partially supported by the Council of Scientific and Industrial Research, India, under Grant No. 01/(1801)/02/EMR-II. S.G thanks JSPS, Japan for the financial support. Thanks are also due to the Chemistry Department, Calcutta University, for allowing us to use the TGA instrument under Department of Science and Technology FIST Program, and to the Indian Institute of Chemical Biology, Calcutta, for the ultracentrifuge facility.

CM049205N

(43) Haneda, K.; Morrish, A. H. *Nature* **1979**, *282*, 186.
(44) Beach, G. S. D.; Parker, F. T.; Smith, D. J.; Crozier, P. A.; Berkowitz, A. E. *Phys. Rev. Lett.* **2003**, *91*, 267201; Novakova, A. A.; Lanchinskaya, V. Y.; Volkov, A. V.; Gendler, T. S.; Kiseleva, T. Y.; Moskvina, M. A.; Zezin, S. B. *J. Magn. Magn. Mater.* **2003**, *258*, 354.
(45) Neel, L. *Ann. Geophys.* **1949**, *5*, 99.
(46) Brown, J. W. F. *Phys. Rev.* **1963**, *130*, 1677.